# Characterization of Concrete Mixes Containing Phase Change Materials

# Characterization of Concrete Mixes Containing Phase Change Materials

**H Paksoy[1], G Kardas[1], Y Konuklu[2], K Cellat[1] and F Tezcan[1]**

[1]Cukurova University, Adana, Turkey
[2]Omer Halisdemir University, Nigde, Turkey

E-mail: hopaksoy@gmail.com

**Abstract**. Phase change materials (PCM) can be used in passive building applications to achieve near zero energy building goals. For this purpose PCM can be added in building structures and materials in different forms. Direct incorporation, form stabilization and microencapsulation are different forms used for PCM integration in building materials. In addition to thermal properties of PCM itself, there are several other criteria that need to be fulfilled for the PCM enhanced building materials. Mechanical properties, corrosive effects, morphology and thermal buffering have to be determined for reliable and long-term applications in buildings. This paper aims to give an overview of characterization methods used to determine these properties in PCM added fresh concrete mixes. Thermal, compressive strength, corrosion, and microscopic test results for concrete mixes with PCM are discussed.

## 1. Introduction

Net-zero energy buildings (NZEBs) are expected to require very low amount of energy and be able to cover significant amount of their energy requirements by renewable energy sources, produced on-site or nearby (1). Recent International Energy Agency Technology Roadmap on Energy Efficient Building Envelopes shows that improvements in the building envelope can reduce total energy consumption in buildings sector by 20% (2). Among the on-site methods that can be used to achieve NZEBs, passive energy technologies used in building envelopes have been attracting interest.

Using phase change materials (PCM) in building materials and structures is one of these passive strategies that can increase energy efficiency and passive use of solar energy (3-6). Concrete is the most common building material used. PCM can be added to concrete in the following different forms.

- Direct integration (7-9)
- Macro-encapsulation (10)
- Microencapsulation (11,12)
- Shape-stabilization (13)

By proper choice of PCM, thermal mass of concrete can be enhanced and indoor temperature can be kept within thermal comfort requirements with limited auxiliary energy requirements for heating and cooling (14,15).

Adding PCM to concrete may affect its porosity, hydration reaction and mechanical strength. The frictional forces in the presence of coarse aggregates in the concrete mix may break the capsules and cause PCM to infiltrate into the porous concrete structure. In such a case the PCM may interact with components of the concrete mix and also rebar causing degradation and corrosion. For reliable application with long lifetime, the effects of adding PCM to concrete mixes have to be determined

with proper characterization methods. This paper gives an overview of characterization methods to determine mechanical, thermal, chemical and microscopic properties of PCM added concrete. Different test results for these properties with relevance to application criteria will be given.

## 2. Materials

The characterization methods that are used and introduced here require different types of samples. For concrete specimens, concrete mix with water : cement ratio of 0.41 was prepared and molded as described in our previous study (7). Eutectic like mixture of fatty acid (FA) containing capric acid (CA) and myristic acid (MA) (75:25 wt.) that was developed in our previous study (7) was used as PCM. A novel microencapsulation of this PCM (mPCM) was done with polystyrene as the shell material in our laboratory with emulsion polymerization method (16). For corrosion test, we reported results with butyl stearate as PCM. The corrosion test results of the fatty acid mix were given in our previous study (17).

## 3. Characterization Methods

### *3.1. Thermal Properties of PCM*

The main criteria for PCM selection are phase change temperature and latent heat. For building applications, thermal comfort zone should be taken into consideration for phase change temperature. International standards for the determination of building thermal comfort are given in ISO 7730 (18) and ASHRAE 55 (19). According to these standards, ideal indoor temperature can be in the range of 22°C – 27°C and PCM should melt within this range. Differential Scanning Calorimeter (DSC) can be used to determine phase change temperature and latent heat of PCMs added to concrete. DSC (Perkin Elmer Diamond) analyses performed for this study operated between 15°C – 35°C at 1°C/min heating/cooling rate in an inert nitrogen atmosphere at 20 mL/min flow rate.

PCMs used should be thermally stable during the preparation and lifetime of concrete mix. Thermal stability of PCM can be determined with Thermogravimetric Analysis (TGA). Results provide information on thermal decomposition behaviour of the PCM. TGA (Perkin Elmer STA 6000) analyses were carried out with 5 mg samples and under inert nitrogen flowing at 20 mL/min. Heating rate was 20°C/min in the range of 30°C – 400°C.

### *3.2. Temperature Evolution of Fresh Concrete*

Temperature of the concrete mix starts increasing as soon as cement and water are introduced to the reactor due to the highly exothermic hydration reaction. Temperature evolution of any concrete in the first 24 hours following mixing has following four stages (20):

I. Dormant – 2–4 h
II. Hardening – 2–4 h
III. Cooling
IV. Densification – setting continues for many years

Reaction products cause cement paste to harden, bond to the coarse and fine aggregates in the concrete mix and become stronger and denser. Any change in the composition of concrete mix may affect the strength and density of the end product. The effects of adding PCM to this process can be observed by a comparative test measuring duration and temperature levels during these four stages. For this purpose, insulated polystyrene containers are used in order to obtain semi-adiabatic conditions for fresh concrete temperature development measurement in the first 24 hours when maximum heat release occurs during hydration reaction of concrete. Two identical containers one with concrete mix with PCM and the other without PCM were prepared. The containers were then placed in a climate chamber (Binder BD) at isothermal temperature of 22°C to eliminate the effect of temperature

fluctuations of ambient. Temperatures were measured at 10 s intervals by T-type thermocouples with accuracy of ±0.5°C and recorded by a data logger (Agilent 34970A).

### *3.3. Thermal Buffering Effect of Concrete*

The aim of using PCM in concrete is to increase thermal mass that will create a buffering effect. This effect will delay the heat gain or loss from the building. For thermal buffering tests, identical cubic concrete specimens with and without PCM with dimensions of 7×7×7 cm were put in constant temperature climate chamber to bring them to the same initial temperature. Specimens were maintained at equilibrium for at least 1 hour prior to testing. Then, specimens were immersed into thermostatic water bath at 30°C, one by one. Temperature development of specimens were measured using T-type thermocouples with an accuracy of ±0.5°C until thermal equilibrium.

Thermal buffering effect can be explained by the delay that occurs in temperature development of the concrete sample. In Equation (1), degree of thermal buffering, $\Delta T_{buffer}$ is given as the temperature difference between the concrete samples with and without PCM (17):

$$\Delta T_{buffer} = T_{c,PCM} - T_{ref} \quad (1)$$

where $T_{c,PCM}$ is temperature of concrete specimen with PCM, $T_{\text{ref}}$ is temperature of reference concrete specimen without PCM.

### *3.4. Compressive Strength Test*

For safe and durable buildings, concrete used should have compressive strengths according to international standards. The compressive strength of hardened concrete samples was determined in accordance with standard TS-EN 12390-3 (21). Standard cubes (15×15×15) were tested after 7 and 28 days of curing in water (20±2°C) using a universal testing machine (Dinc Makina D201A). Before the compression test, the surface of the compression machine was cleaned, and the specimens were placed by aligning the axis with the centre of thrust of the plate. The test machine applied the load gradually at the rate of approximately 0.6 MPa/s until the specimen could carry no further load, and failure occurred. The compressive stresses were calculated in MPa from the respective maximum loads sustained by the cubes before they failed.

### *3.5. Corrosion*

The corrosion is another property that should be considered when phase change materials (PCM) are added to concrete for building applications. PCM may increase the energy efficiency, but the corrosion resistance of the steel in concrete (rebar) can decrease. The corrosion effect of PCM on rebar should be determined and controlled for long-term durable PCM building applications. Corrosion behavior can be monitored in any period of time by using electrochemical measurements such as electrochemical impedance spectroscopy (EIS) and open circuit potential (Eocp).

Electrochemical measurement was conducted using the conventional three-electrode system. The rebar, Ag/AgCl (3.0 M KCl) and Pt sheet were used as working, reference and counter electrodes, respectively. The electrode surfaces, except for the exposed one, were coated with polyester block in order to examine the sample corrosion behavior only. The concrete mix prepared according to the standards was put in cubical molds with dimension of 7x7x7 cm. The rebar specimens were located at the center of the cubical mold to allow diffusion of ions from the electrolyte to the electrode surface to be at equal distances in all directions. The molded specimens were kept at room temperature for 24 h before being de-molded and cured in water at 20±2°C for 28 days. Cured specimens were then fully immersed in 3.5% wt NaCl (analytical grade, Sigma Aldrich) electrolyte for electrochemical measurements at room condition. Three parallel specimens were prepared and measured to determine the uncertainty of the measurement. The EIS experiments were carried out utilizing CHI 660 D electrochemical analyzer (serial number F1190) at open circuit potential between 100 kHz and 0.0046 Hz for 240 days with amplitude of 5 mV.

*3.6. Microscopic Properties*

Microscopic properties showing geometry, shape, particle size and distribution are important especially when microencapsulated PCMs are used together with concrete. Among the microscopic methods Field Emission Scanning Electron Microscope – FESEM is commonly used for this purpose. This analysis can shed information on the following characteristics:

- Homogeneous distribution of microencapsulated PCM in concrete
- Robustness of shell structure of microencapsulated PCM
- Particle size and uniformity of microencapsulated PCM
- Effect of microencapsulated PCM on micro structure of concrete
- Corrosion effects of PCM on steel bar in concrete

Samples were prepared for FESEM (Zeiss/Supra 55) analysis by covering with platinum utilizing a plasma coater to increase conductivity. FESEM measurements were carried out at an extra-high tension (EHT) of 20 kV.

## 4. Results and Discussion

*4.1. Thermal Properties of PCM*

DSC of the fatty acid mixture for building application was given in our previous study (16). The melting range of 20.14 – 28.03°C was determined from the on-set and end temperatures on the melting curve and latent heat of melting as 148.5 J/g. On the freezing curve, the phase change temperature range was observed to shift to 10.00 – 15.69°C and latent heat of freezing remained almost the same as 149.1 J/g. This shift in on-set and end temperatures shows this mixture has hysteresis. This difference is also defined as degree of supercooling by Zhang et al. (22) and can be more enhanced in the mg sized samples of DSC. For this mixture the difference in on-set temperatures was 4.45°C (16).

Before mixing into concrete, PCM is microencapsulated in polymer shell. Microencapsulation decreases the latent heat of the original PCM. Figure 1 shows the DSC of microencapsulated fatty acid mixture. The melting range is 25.32 – 17.10°C and melting latent heat is 90.8 J/g. The difference in on-set temperature has decreased to 1.79°C, which indicates that microencapsulation decreases supercooling behavior.

DSC results can also be used to determine the encapsulation % according to Equation (2):

$$Encapsulation\% = \frac{\Delta H_{mPCM}}{\Delta H_{PCM}} \times 100 \quad (2)$$

where $\Delta H_{PCM}$ and $\Delta H_{mPCM}$ are the latent heat of PCM and microencapsulated PCM. The encapsulation percentage calculated using latent heats of melting according to Equation (2) is 61.1%.

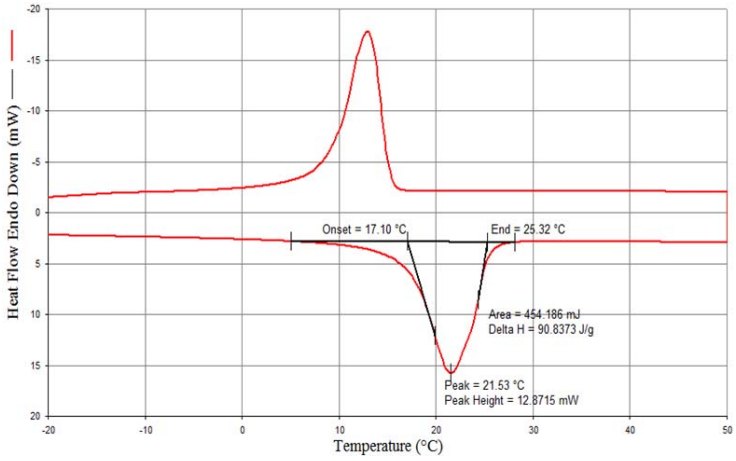


**Figure 1**. DSC of microencapsulated PCM (23).

Thermal stability of fatty acid mixture and microencapsulated PCM is compared with TGA analysis shown in Figure 2. The TGA curve of the fatty acid mixture shows it is decomposing in a single step with first decomposition temperature of 150°C and final temperature of 250°C at which sample decomposes with no residues. For microencapsulated PCM, there are two steps; the first one corresponding to the fatty acid mixture in the capsule, which is the same as the fatty acid mixture alone. The second one corresponds to the polymer shell of the microcapsule decomposing at 250°C and final decomposition temperature is at 450°C. This shows that microencapsulation increases thermal durability of the fatty acid mixture by about 200°C.

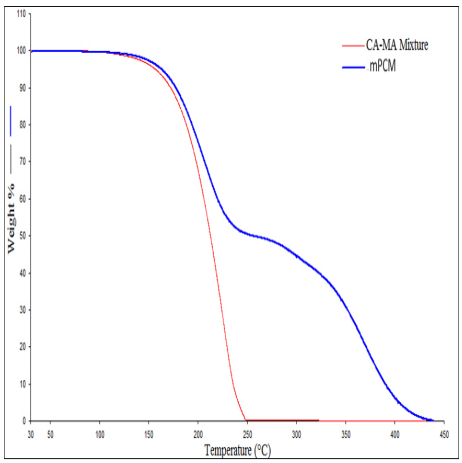


**Figure 2.** TGA of fatty acid mixture (CA-MA mixture) and mPCM (23).

*4.2. Temperature Evolution of Fresh Concrete*

Temperature changes in the first 24 h of fresh concrete with 1% and 3% of PCM and without (reference) are compared in Figure 3 from our previous study (17). Different stages of temperature evolution as explained in the previous section are also shown on this figure. The samples with PCM content have lower maximum temperatures by about 1°C compared to the reference. Maximum temperature on this curve decreases at higher PCM contents. Another important information from this figure is during cooling stage, the samples with PCM have lower temperatures until around 23°C that corresponds to melting temperature of PCM. The lower temperature evolution during the cooling stage may avoid cracks that can be seen in concrete especially during warm weather. Implications of adding PCM on hydration reaction and densification mechanism needs further research.

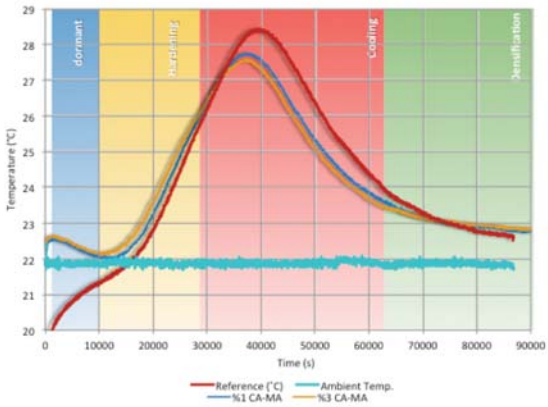


**Figure 3**. Temperature evolution in the first 24 hours of fresh concrete (17).

*4.3. Thermal Buffering Effect of Concrete*

Degree of thermal buffering, $\Delta T_{buffer}$ calculated from Eqn(1) using data from temperature distribution of concrete samples in thermostatic bath (Figure 4-a) as explained in the previous section is shown in Figure 4-b (17). The composition of PCM and microencapsulated PCM in concrete were 2% and 10% by weight, respectively. These compositions were used to stay within allowable limits of compressive strengths. The amount of PCM in the concrete with microencapsulated PCM was about twice compared to the PCM only form. The maximum $\Delta T_{buffer}$ was measured as 5.0°C and 3.8°C for microencapsulated PCM and PCM, respectively. The higher amount of PCM increased degree of thermal buffering by 1.2°C (17).

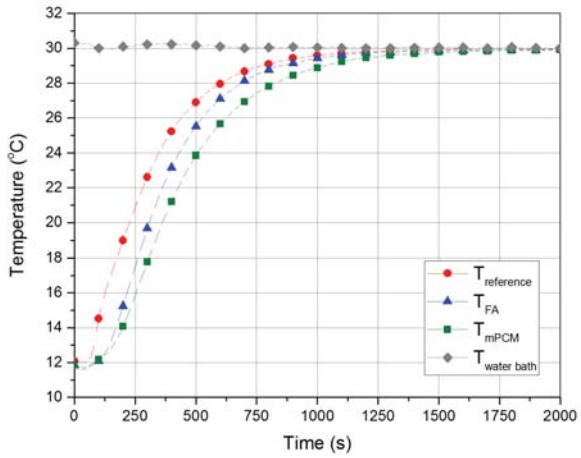


(a)

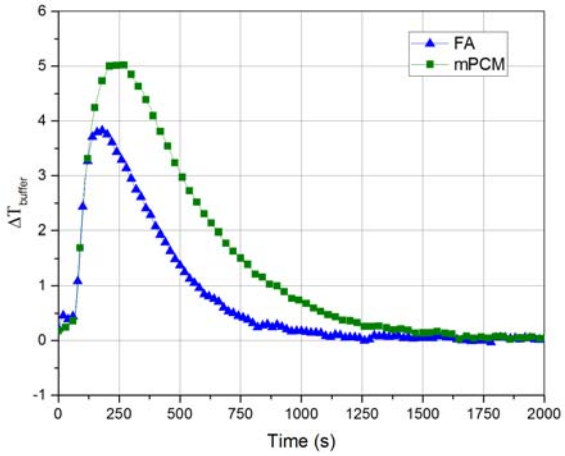


(b)

**Figure 4.** (a) Temperature change of concrete samples in thermostatic bath at 30°C (b) Change of degree of thermal buffering, $\Delta T_{buffer}$ (17).

*4.4. Compressive Strength*

Addition of PCM in both bulk and microencapsulated forms decreases compressive strength of concrete as seen in Figure 5 (17). As expected, the compressive strengths after 7 days of curing were lower than 28 days of curing. The compressive strength after 28 days decreased more for concrete with 10% microencapsulated PCM with a reduction value of 38%. For concrete with 2% PCM reduction value was 28%. This reduction is a result of replacing aggregates with PCM, which is a main challenge of incorporating PCM into concrete. In the compressive strength test results given here (19) high strength concrete formulation (C40/50) was used in order to determine the limiting compressive strength that can be achieved. Even after reduction, concrete samples with both of PCMs comply with C30/37 class of concrete according to TS EN 206-1 (24), which renders them usable even for earthquake zones.

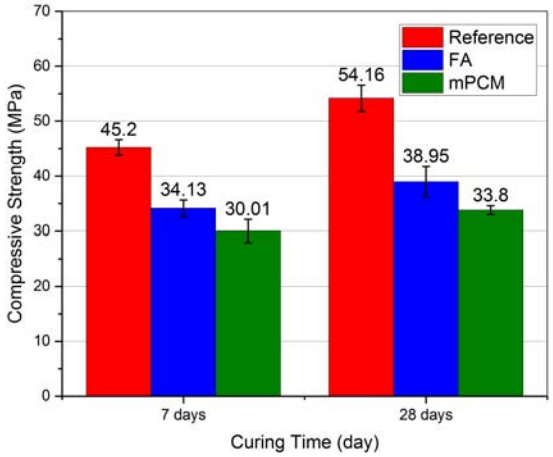


**Figure 5.** Effects of adding PCM to compressive strength of concrete (17).

*4.5. Corrosion*

The long-term corrosion behavior can be tested by analyzing Eocp values in aggressive media. Eocp is defined as the sample potential with respect to the reference electrode when no current is applied. The Eocp value depends on resistivity, porosity, film thickness, oxygen diffusion through the pores, corrosion products and surroundings of the sample (25). The conventional standard method for the

description of corrosion behavior of samples is ASTM C876-99 (26). This method gives evidence on the degree of probability of corrosion of the sample according to the following three regions of Eocp:

I. 10% probability of corrosion for Eocp > -0.119 V vs. Ag/AgCl
II. uncertainty of corrosion for -0.119 V < Eocp< -0.269 V vs. Ag/AgCl
III. 90% probability of corrosion for Eocp < -0.269 V vs. Ag/AgCl

In our previous study, effects of corrosion behavior of rebar in concrete with fatty acid additive using the electrochemical method given here was reported (19). Results from corrosion test of butyl stearate (BS) as PCM added concrete mix is given here. Eocp values of rebar is shown in Figure 6. The corrosion probability regions are given according to ASTM C876-99 standard as explained above. Eocp values were 0.011 mV and -0.174 mV for rebar and rebar-BS at the end of one hour. Eocp values of rebar oscillated between uncertainty of corrosion and 90% probability of corrosion regions with a widespread range of potential values during 210 days. For rebar-BS, Eocp values varied in a narrow range with little fluctuations between uncertainty of corrosion and 90% probability of the corrosion regions. This method demonstrates that rebar-BS electrode has lower probability of corrosion compared to rebar electrode in %3.5 wt during 210 days.

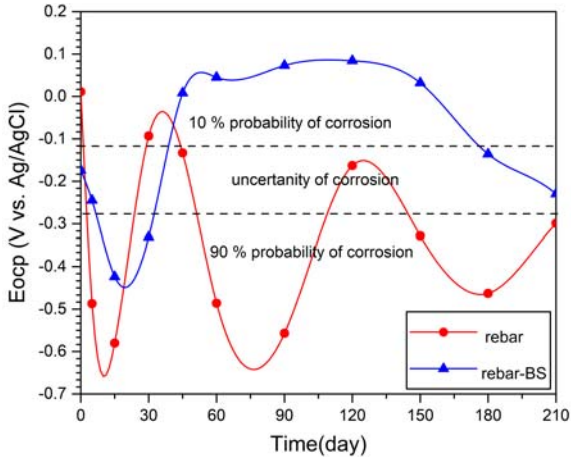


**Figure 6.** The Eocp values of rebar and rebar-BS during 210 days.

Corrosion behavior of rebar can be further investigated in detail with the electrochemical impedance spectroscopy (EIS) technique. EIS measurements are widely utilized in order to explain corrosion process mechanism of rebar, diffusion of corrosion products and especially chloride ions to and from electrode surface, film coverage on electrode and solution resistance. EIS, with these aspects, is a comprehensive electrochemical investigation technique. Nyquist's plot from EIS measurement is given in Figure 7. The plot has one depressed semi circle in high-frequency region and followed by straight line in the low-frequency region. The high-frequency semi circle is associated with the charge transfer resistance (Rt), accumulation resistance (Ra) and film resistance (Rf), which can only be seen in the presence of PCM. The straight line in the low-frequency region is ascribed with the diffusion-controlled corrosion process on the electrode surface. The diffusion resistance (Rd) consists of diffusion of various types of ions, such as chloride and corrosion products within the concrete pores (27). Chloride ions with higher concentration in the electrolyte automatically diffuse through concrete pores towards the electrode surface, at the same time, corrosion products are formed on the electrode surface, which move towards electrolyte to stabilize concentration differences in both zones. The solution resistance (Rs) is related to chloride ions going into solution through concrete pores to the electrode surface. The change of concrete porosity with additives can be explained with magnitude of Rs. The higher *R*s values of the electrode means lower porosity of concrete. The calculated Rs values from Figure 7 were 643 Ω $cm^2$ and 1493 Ω $cm^2$ for rebar-BS and rebar electrodes. These Rs values show that the concrete porosity increases with BS addition to the concrete.

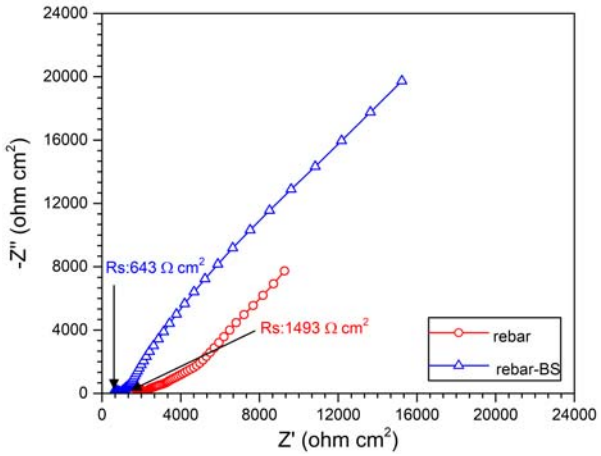


**Figure 7.** Nyquist plot of rebar and rebarBS electrode in % 3.5 NaCl solution at the room temperature after 210 days.

*4.6. Microscopic Properties*

The SEM images given in Figure 8 are taken from the broken concrete specimens that included 10% microencapsulated PCM. In the Figure 8-a at the 30 000 magnification the specific micro-crystal structures (28) of Ettrengit and C-S-H can easily be detected. This shows that addition of microencapsulated PCM did not change the micro-structure of concrete. In Figure 8-b showing the same sample at 150 000 magnification confirms that microcapsules are not broken and kept their spherical geometries after being mixed and even after breaking of the concrete specimen. The size of the microcapsules that can be detected from Figure 8-b is in the range of 60-160 nm.

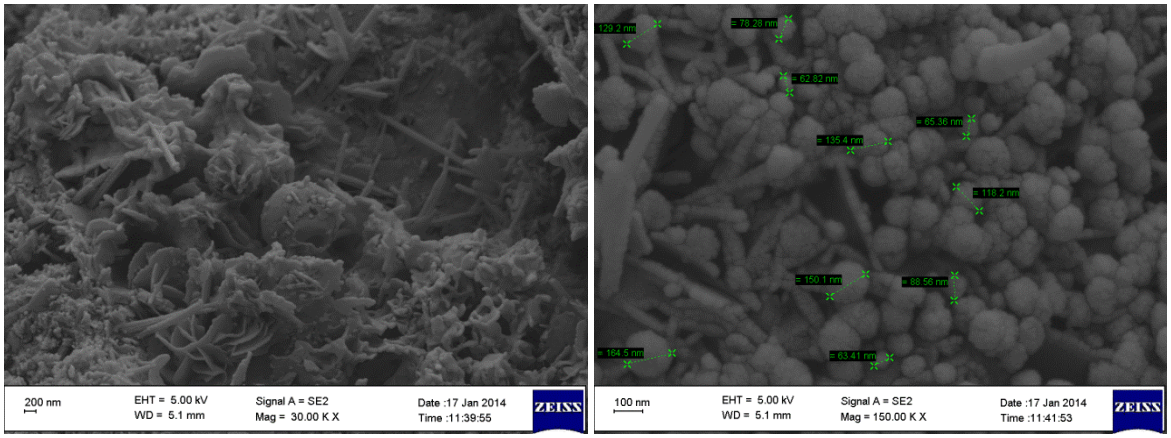


(a) (b)

**Figure 8.** SEM images of broken concrete specimen with microencapsulated PCM (a) at 30 000 magnification (b) at 150 000 magnification.

## 5. Conclusions

Passive PCM applications in buildings can increase energy efficiency and savings to help in meeting challenging NZEB goals. The effects of adding PCM to concrete have to be determined for sustainability and security. For characterization of PCMs and PCM in concrete conventional methods DSC, TGA for thermal properties, compressive strength measurement for mechanical properties and FESEM for microscopic structure have been used. In addition to these new methods for determining

thermal buffering effect, fresh concrete temperature evolution and electrochemical methods for the corrosive effects of PCM on rebar in concrete have been developed and introduced. The results confirm that the fatty acid mixture (capric acid and myristic acid) used as PCM in this study can enhance thermal mass of concrete without degradation and compressive strength was kept within standards. Microencapsulated PCMs with polystyrene shells were safely added to concrete and the main micro-structural elements of concrete and morphology of microcapsules were not affected. Long-term corrosive effect of the PCM on concrete rebar can be easily determined with the electrochemical introduced here. The results of electrochemical methods can also give information on the change of porosity of the PCM added concrete, which has links to the mechanical durability of concrete. Increase of thermal buffering effect of fresh concrete with PCM addition can be quantified with the new method introduced here. For the fatty acid mixture amounts used here, the degree of thermal buffering can be increased by 1.2°C. in These characterization methods are recommended for determining applicability of PCMs to concrete and expected long-term behavior. More methods for determining flammability, thermal mass analysis and other mechanical properties of concrete with PCM are also needed. For further studies detailed kinetic analysis of hydration reaction when PCM is added to concrete can be done. Temperature evolution in the first 24 h shows that maximum temperature attained when PCM is added is lower, which can indicate a cooling effect. This condition has to be further investigated.

**Acknowledgements**
The authors would like to acknowledge the funding provided by the European Union's Horizon 2020 research and innovation programme under grant agreement No 657466 (INPATH-TES).

**References**

[1] European Commission, Energy Performance of Buildings Directive (recast 2010/31/EU), European Parliament, 2010
[2] International Energy Agency Technology Roadmap on Energy Effiicient Building Envelopes, IEA Publications, 2013.
[3] Tyagi, V. V., & Buddhi, D. (2007). PCM thermal storage in buildings: a state of art. Renewable and Sustainable Energy Reviews, 11(6), 1146-1166.
[4] Kuznik, F., David, D., Johannes, K., Roux, J.-J. (2011) A review on phase change materials integrated in building walls, Renew. Sustain. Energy Rev. 15 379–391.
[5] Akeiber H, Nejat P, Majid MZA, Wahid MA, Jomehzadeh F, Famileh IZ. (2016). A review on phase change material (PCM) for sustainable passive cooling in building envelopes. Renewable and Sustainable Energy Reviews; 60:1470–97.
[6] Ling, T. C., Poon, C. S. (2013). Use of phase change materials for thermal energy storage in concrete: An overview. Construction and Building Materials, 46, 55-62.
[7] Cellat, K., Beyhan, B., Gungor, C., Konuklu, Y., Karahan, O., Dundar, C., Paksoy, H. (2015). Thermal enhancement of concrete by adding bio-based fatty acids as phase change materials, Energy and Buildings, 106, 156-163
[8] Zhang, Z., Shi, G., Wang, S., Fang, X., Liu, X. (2013) Thermal energy storage cement mortar containing n-octadecane/expanded graphite composite phase change material, Renewable Energy 50 670–675.
[9] Xu, B., Li, Z. (2013) Paraffin/diatomite composite phase change material incorporated cement-based composite for thermal energy storage, Appl. Energy 105 229–237.
[10] Vicente, R., Silva, T. (2014) Brick masonry walls with PCM macrocapsules: an experimental approach, Appl. Therm. Eng. 67 24–34.
[11] Konuklu, Y., Ostry, M., Paksoy, H.O., Charvat, P. (2015) Review on using microencapsulated phase change materials in buildings, Energy and Buildings 106 134–155
[12] Cabeza, L. F., Castellon, C., Nogues, M., Medrano, M., Leppers, R., Zubillaga, O. (2007). Use of microencapsulated PCM in concrete walls for energy savings. Energy and Buildings,

39(2), 113-119.
[13] Cao, L, Tang, F, Fang, G. (2014) Synthesis and characterization of microencapsulated paraffin with titanium dioxide shell as shape stabilized thermal energy storage materials in buildings. Energy and Buildings 72:31–7.
[14] Biswas, K., Abhari, R., (2014) Low-cost phase change material as an energy storage medium in building envelopes: Experimental and numerical analyses, Energy Conversion and Management, 88, 1020-1031
[15] Soares, N., Costa, J.J., Gaspar, A.R., Santos, P. (2013) Review of passive PCM latent heat thermal energy storage systems towards buildings' energy efficiency, Energy Build. 59 82–103.
[16] Beyhan, B., Cellat, K., Konuklu, Y., Gungor, C., Karahan, O., Dundar, C., Paksoy, H. (2017). Robust microencapsulated phase change materials in concrete mixes for sustainable buildings. Int. J. Energy Res. 41:113–126.
[17] Cellat, K., Tezcan, F., Beyhan, B., Kardas, G., Paksoy, H. (2017) A comparative study on corrosion behavior of rebar in concrete with fatty acid additive as phase change material, Construction and Building Materials, 143 490-500.
[18] Iso, En., 7730: 2005:"Ergonomics of the Thermal Environment – Analytical Determination and Interpretation of Thermal Comfort Using Calculation of the PMV and PPD Indices and Local Thermal Comfort Criteria", International Organization for Standardisation, Geneva, 2005.
[19] ASHRAE/ANSI, Standard 55-2004, Thermal Environmental Conditions for Human Occupancy, American Society of Heating, Refrigerating and Air-Conditioning Engineering, Atlanta, GA, 2004.
[20] Taylor, P.C., Kosmatka, S.H., Voigt, G.F. (2006) Integrated materials and construction practices for concrete pavement: A state-of-the-practice manual.
[21] TS EN 12390-3 (2002). Testing hardened concrete - Part 4: Compressive strength of test specimens. Turkish Standards Institution, Ankara (in Turkish)
[22] Zhang, X., Z, Fan, Y., Tao, X., Yick, K. (2005) Crystallization and prevention of supercooling of microencapsulated nalkanes. Journal of Colloid and Interface Science 281:299–306
[23] Beyhan,B., Cellat, K., Paksoy, H., Konuklu, Y., Karahan, O., Dundar, C., Gungor, C. (2015) New Microencapsulated Phase Change Material for Thermal Energy Storage in Building Applications, GREENSTOCK2015 "13TH International Conference on Energy Storage", Beijing, China
[24] TS EN 206-1, Concrete-Part 1: Specification, Performance, Production and Conformity, Turkish Standards Institution, Ankara, 2014 (in Turkish).
[25] Verma, S.K., Bhadauria, S.S., Akhtar. (2014) Monitoring corrosion of steel bars inreinforced concrete structures, Sci. World J.
[26] ASTM C876-91(1999), Standard Test Method for Half-Cell Potentials of Uncoated Reinforcing Steel in Concrete (Withdrawn 2008), ASTM International, West Conshohocken, PA.
[27] R. Vedalakshmi, V. Saraswathy, H.-W. Song, N. Palaniswamy. (2009) Determination of diffusion coefficient of chloride in concrete using Warburg diffusion coefficient, Corros. Sci. 51 (6) 1299–1307
[28] Coatanlem P, Jauberthie R, Rendell F. Lightweight wood chipping concrete durability. Construct Build Mater 2006; 20:776–81.